Anal. Calcd for $C_{24}H_{24}Cl_2Zr$: C, 60.74; H, 5.10. Found: C, 60.35; H, 4.98.

Racemic [Ethylenebis(η^5-4,7-dimethylindenyl)]zirconium Dichloride (5c). This compound was prepared under different conditions than that reported above: A suspension of compound 2c (166.3 mg, 0.53 mmol) in dry DME (10 mL) was cooled to 0 °C under argon. A solution of *n*-butyllithium in hexane (0.47 mL, 2.5 M, 2.2 equiv) was added dropwise, via syringe, over 10 min. The mixture was warmed to room temperature; the indene dissolved with formation of a yellow solution, and, after 45 min at room temperature, a colorless precipitate separated. In a separate flask, $ZrCl_4$ (123.0 mg, 0.53 mmol) was treated with 5 mL of DME at -78 °C. The solution was then warmed to room temperature and then added dropwise, using a syringe pump, to the suspension of the dianion in DME over a period of 1.5 h. The dianion gradually dissolved and a yellow solution with some precipitate was obtained. The mixture was stirred overnight at 25 °C. Ethereal HCl was added via syringe (1.0 mL of 0.3 M) and the mixture concentrated in vacuo. The residue was taken up in ether and filtered, washing with small volumes of ether. The yellow solid was washed with 6 M HCl, water, ethanol, and then ether as described above and dried in vacuo (63 mg, 25% yield). The crude product was obtained as a single stereoisomer and could be purified by crystallization from hexanes–toluene. IR (KBr) 3080, 3027, 2934, 2888, 2854, 1601, 1495, 1451 s, 1379, 1328, 1096, 1068, 1005, 926, 816 s, 745, 663, 634 cm^{-1}; ^1H NMR (200 MHz, $CDCl_3$) δ 6.81–6.75 (two overlapping d, J = 3.5, 7.8 Hz, total 4 H), 6.62 (d, J = 7.8 Hz, 2 H), 5.90 (d, J = 3.5 Hz, 2 H), 3.5 (AA′ multiplet, 2 H), 3.0 (BB′ multiplet, 2 H), 2.34 (s, 6 H), 2.24 (s, 6 H); ^{13}C NMR (50 MHz, $CDCl_3$) δ 132.9, 130.1, 128.7, 128.4, 125.4, 125.2, 121.5, 113.3, 112.7, 30.3, 21.4, 18.6; MS (EI) 472 (M^+, $^{90}Zr^{35}Cl_2$). Anal. Calcd for $C_{24}H_{24}Cl_2Zr$: C, 60.74; H, 5.10. Found: C, 60.41; H, 5.32.

Racemic [Ethylenebis(η^5-5,6-dimethoxyindenyl)]zirconium Dichloride (5d). This compound was prepared in 24% yield and was obtained free of a minor amount of its meso isomer by washing the final product with hot toluene. IR (KBr) 3079, 3061, 2993, 2958, 2931, 2898, 2830, 1621, 1528, 1493, 1458, 1428, 1384, 1370, 1314, 1239, 1224, 1207, 1185, 1147, 1054, 1028, 1017, 997, 977, 901, 875, 851, 839, 827, 798, 728, 530, 454, 420 cm^{-1}; ^1H NMR (200 MHz, $CDCl_3$) δ 6.73 (s, 2 H), 6.71 (s, 2 H), 6.45 (d, J = 3.3 Hz, 2 H), 5.98 (d, J = 3.3 Hz, 2 H), 3.96 (s, 6 H) 3.93 (s, 6 H), 3.64 (AA′BB′ m, 4 H); ^{13}C NMR (50 MHz, CD_2Cl_2) δ 154.4, 152.5, 125.9, 121.0, 119.5, 110.4, 109.8, 102.6, 98.9, 56.4, 56.4, 29.0; MS (EI) 536 (M^+, $^{90}Zr^{35}Cl_2$). Anal. Calcd for $C_{24}H_{24}Cl_2O_4Zr$: C, 54.54; H, 4.49. Found: C, 54.62; H, 4.90.

Acknowledgment. We thank the Natural Sciences and Engineering Research Council and Nova Corp. of Alberta for financial support of this work.

OM910798I

Photochemical Reactions of $Cp_2Fe_2(CO)_4$ with $HSnBu_3$

Shulin Zhang and Theodore L. Brown*

School of Chemical Sciences, University of Illinois at Urbana Champaign, Urbana, Illinois 61801

Received December 30, 1991

The photochemical reactions of $Cp_2Fe_2(CO)_4$ with $HSnBu_3$ in hexane solutions have been studied by employing continuous or flash photolysis methods. The primary reaction products, $Cp(CO)_2FeH$, $Cp(CO)_2FeSnBu_3$, and $Cp(CO)Fe(H)(SnBu_3)_2$, have been independently synthesized and characterized by elemental analysis and NMR or IR spectroscopy. Under an Ar or CO atmosphere, the amount of $Cp(CO)_2FeH$ formed in the early stage of the reaction is always in a 1:1 molar ratio with the total amount of $Cp(CO)_2FeSnBu_3$ and $Cp(CO)Fe(H)(SnBu_3)_2$, and in a 1:1 molar ratio with the loss of $Cp_2Fe_2(CO)_4$. The rate for the continuous photolysis reaction is inversely related to CO partial pressure. The results rule out pathways involving the intermediacy of the $Cp(CO)_2Fe^{\bullet}$ radical. The behavior of the system is consistent with a reaction pathway that involves oxidative addition of $HSnBu_3$ to the CO-loss intermediate, $Cp_2Fe_2(\mu\text{-}CO)_3$. The second-order rate constant for oxidative addition of $HSnBu_3$ to $Cp_2Fe_2(\mu\text{-}CO)_3$ is 1.26×10^5 M^{-1} s^{-1} at 25 °C. The subsequent elimination of $Cp(CO)_2FeH$ obeys a first-order rate law with an apparent rate constant of $\sim 2 \times 10^{-2}$ s^{-1}.

Introduction

It has been well established that the photochemistry of metal–metal-bonded carbonyls involves both homolysis of the metal–metal bond, which generates 17-electron radicals, and cleavage of the metal–CO bond, which produces a CO-loss intermediate.[1,2] The reactions of the 17-electron radicals,[3-7] e.g., electron and atom transfer, recombination, ligand addition, and substitution, have been the focus of studies for some years. More recently there has been increased awareness of the importance of the dinuclear intermediates resulting from CO loss.

$Cp_2Fe_2(CO)_4$ has a very diverse photochemistry.[1,2] Photochemical generation of the radical $Cp(CO)_2Fe^{\bullet}$ and the CO-loss species $Cp_2Fe_2(CO)_3$ has been established.[1,2,8-11] Two isomers of the CO-loss species have been identified;

(1) Geoffroy, G. L.; Wrighton, M. S. *Organometallic Photochemistry*; Academic Press: New York, 1979.
(2) Meyer, T. J.; Caspar, J. V. *Chem. Rev.* **1985**, *85*, 187.
(3) (a) Brown, T. L. *Ann. N.Y. Acad. Sci.* **1980**, *333*, 80. (b) Brown, T. L. In *Organometallic Radical Processes*; Trogler, W. C., Ed.; Elsvier: Amsterdam, 1990; p 67. (c) Trogler, W. C. *Int. J. Chem. Kinet.* **1987**, *19*, 1025.
(4) Baird, M. C. In *Organometallic Radical Processes*; Trogler, W. C., Ed.; Elsvier: Amsterdam, 1990; p 49.
(5) (a) Kochi, J. K. In *Organometallic Radical Processes*; Trogler, W. C., Ed.; Elsvier: Amsterdam, 1990; p 201. (b) Kochi, J. K. *J. Organomet. Chem.* **1986**, *300*, 139.
(6) (a) Stiegman, A. E.; Tyler, D. R. *Comments Inorg. Chem.* **1986**, *5*, 215. (b) Tyler, D. R. In *Organometallic Radical Processes*; Trogler, W. C., Ed.; Elsvier: Amsterdam, 1990; p 338. (c) Tyler, D. R. *Acc. Chem. Res.* **1991**, *24*, 325.
(7) Astruc, D. *Chem. Rev.* **1988**, *88*, 1189.
(8) Caspar, J. V.; Meyer, T. J. *J. Am. Chem. Soc.* **1980**, *102*, 7794.
(9) Hepp, A. F.; Blaha, J. P.; Lewis, C.; Wrighton, M. S. *Organometallics* **1984**, *3*, 174.
(10) (a) Hooker, R. H.; Mahmoud, K. A.; Rest, A. J. *J. Chem. Soc., Chem. Commun.* **1983**, 1022. (b) Hooker, R. H.; Rest, A. J. *J. Chem. Soc., Dalton Trans.* **1990**, 1211. (c) Bloyce, P. E.: Campen, A. K.; Hooker, R. H.; Rest, A. J.; Thomas, N. R.; Bitterwolf, T. E.; Shade, J. E. *J. Chem. Soc., Dalton Trans.* **1990**, 2833.
(11) (a) Moore, B. D.; Simpson, M. B.; Poliakoff, M.; Turner, J. J. *J. Chem. Soc., Chem. Commun.* **1984**, 972. (b) Moore, B. D.; Simpson, M. B.; Poliakoff, M.; Turner, J. J. *J. Phys. Chem.* **1985**, *89*, 850. (c) Dixon, A. J.; Healy, M. A.; Poliakoff, M.; Turner, J. J. *J. Chem. Soc., Chem. Commun.* **1986**, 994. (d) Dixon, A. J.; Gravelle, S. J.; van de Burgt, L. J.; Poliakoff, M.; Turner, J. J. *J. Chem. Soc., Chem. Commun.* **1987**, 1023.

0276-7333/92/2311-2122$03.00/0

$Cp_2Fe_2(\mu\text{-}CO)_3$, which contains three symmetrically bridged CO groups,[9-12] and $Cp_2Fe_2(\mu\text{-}CO)_2(\mu\text{-}\eta^1,\eta^2\text{-}CO)$ in which one of the CO acts as a 4-electron donor ligand.[13] The reactions of $Cp_2Fe_2(CO)_4$ with hydrogen, silanes, and tin hydrides (H–X, X = H, SiR_3, SnR_3) produce catalytically active intermediates in hydrogenation, hydroformylation, hydrosilation,[14-16] and hydrostannation, respectively. Three possible pathways can be considered to be involved in these reactions.

1. H atom transfer to $Cp(CO)_2Fe^\bullet$:

$$Cp(CO)_2Fe^\bullet + H\text{–}X \rightarrow Cp(CO)_2Fe(H) + X^\bullet \quad (1)$$

$$Cp(CO)_2Fe^\bullet + X^\bullet \rightarrow Cp(CO)_2Fe(X) \quad (2)$$

$$X^\bullet + X^\bullet \rightarrow X_2 \quad (3)$$

2. Oxidative addition to $Cp(CO)_2Fe^\bullet$:

$$Cp(CO)_2Fe^\bullet + H\text{–}X \rightarrow Cp(CO)Fe(H)(X)^\bullet + CO \quad (4)$$

$$Cp(CO)Fe(H)(X)^\bullet + H\text{–}X \rightarrow Cp(CO)Fe(H)_2(X) + X^\bullet \quad (5)$$

$$Cp(CO)Fe(H)_2(X) \rightarrow Cp(CO)Fe(X) + H_2 \quad (6)$$

$$Cp(CO)Fe(X) + CO \rightarrow Cp(CO)_2Fe(X) \quad (7)$$

$$Cp(CO)Fe(X) + H\text{–}X \rightleftharpoons Cp(CO)Fe(H)(X)_2 \quad (8)$$

$$Cp(CO)Fe(H)_2(X) \rightleftharpoons Cp(CO)Fe(H) + H\text{–}X \quad (9)$$

$$Cp(CO)Fe(H) + CO \rightarrow Cp(CO)_2Fe(H) \quad (10)$$

3. Oxidative addition to $Cp_2Fe_2(CO)_3$:

$$Cp_2(CO)_3Fe_2 + H\text{–}X \rightarrow Cp_2(CO)_3Fe_2(H)(X) \quad (11)$$

$$Cp_2(CO)_3Fe_2(H)(X) \rightarrow Cp(CO)_2Fe(H) + Cp(CO)Fe(X) \quad (12)$$

$$Cp_2(CO)_3Fe_2(H)(X) \rightarrow Cp(CO)_2Fe(X) + Cp(CO)Fe(H) \quad (13)$$

followed by reactions 7–10

The photochemical reactions of $Mn_2(CO)_8L_2$ (L = CO, PR_3; R = alkyl) with $HSnBu_3$ have been investigated recently in this laboratory.[17] The oxidative addition of $HSnBu_3$ to the CO-loss intermediate, $Mn_2(CO)_8(\mu\text{-}\eta^1,\eta^2\text{-}CO)$, was found to be the only significant reaction pathway. In this contribution we report on studies of the photochemical reactions of $Cp_2Fe_2(CO)_4$ with $HSnBu_3$, in which the three outlined pathways and additional subsequent reactions seem reasonable possibilities. We have employed continuous photolysis to determine the reaction products and product distribution, and flash photolysis studies to directly probe the kinetics of the reaction intermediates. These observations shed important light on our understanding of the detailed course of an overall reaction that involves several short-lived intermediates.

Experimental Section

All experiments were carried out under an atmosphere of purified argon employing Schlenk techniques or were performed in a glovebox. Infrared spectra were recorded on a Perkin-Elmer 1710 FTIR spectrometer (2-cm^{-1} resolution) using 1.0-mm KCl solution cells with Teflon stoppers. ^1H and ^{13}C NMR spectra were recorded on a Varian XL-200 or U400 spectrometer using samples in flame-sealed NMR tubes. Elemental analyses were performed in the micoanalytical laboratory of the School of Chemical Sciences, University of Illinois.

Materials. $Cp_2Fe_2(CO)_4$ (Strem Chemicals) and $ClSnBu_3$ (Aldrich) were used without further purifications. $HSnBu_3$ (Aldrich) was distilled over $LiAlH_4$ (65 °C, 0.3 mmHg). Tetrahydrofuran (THF, Fisher Scientific) and C_6D_6 (Aldrich) were distilled after refluxing with CaH_2 overnight under Ar.

n-Hexane (Burdick and Jackson) was purified by stirring with concentrated sulfuric acid for at least 7 days followed by washing with water four times. After drying over anhydrous $CaCl_2$, it was passed through a column of freshly activated silica gel, refluxed over CaH_2, and distilled under Ar. It was then subjected to three freeze–pump–thaw cycles and stored over activated 4-Å molecular sieves in a flask fitted with a threaded Teflon stopcock.

Carbon monoxide (Matheson Gas Products, Matheson purity grade, 99.99+%) was purged of $Fe(CO)_5$ by passage through a copper tube packed with activated charcoal heated to 180 °C in a sand bath, followed by passage through a second charcoal-packed copper tube cooled in a dry ice–ethanol bath. The CO was then passed through 4-Å molecular sieves and an O_2 trap (American Scientific).

Argon (research grade) and hydrogen obtained from Linde Specialty Gas Co. were purified by passing through MnO and 4-Å molecular sieve columns.

Continuous Photolysis Procedures. The light source used in continuous photolysis reactions was a 275-W General Electric sunlamp (predominantly 366-nm radiation). After freeze–pump–thaw degassing of a reaction solution (typically 10 mL) in a 30-mL Schlenk tube with a threaded Teflon stopcock, the solution was filled with Ar, CO, or Ar/CO gas mixtures. The solution was then irradiated by placing the sunlamp 10 cm away from the reaction tube. The reaction temperature was maintained at ca. 30 °C by using a fan. Progress of the reactions was monitored using IR spectra of samples withdrawn from the reaction solution.

$Cp(CO)_2FeH$ was prepared in solution by sunlamp photolysis of 10 mL of a 1.25 mM hexane solution of $Cp_2Fe_2(CO)_4$ under 1 atm of H_2. After 70 min of photolysis, about 50% of $Cp_2Fe_2(CO)_4$ had been consumed, based on the IR spectrum. New bands at 2023 and 1966 cm^{-1}, ascribed to $Cp(CO)_2FeH$,[15,18] were observed. No other CO stretching bands were seen in the IR spectra, and no solid material was found in the reaction solution. We thus assume $Cp(CO)_2FeH$ is the only product under the conditions employed. The extinction coefficients of $Cp(CO)_2FeH$ at 2023 cm^{-1} (ϵ = 608 mm^{-1} M^{-1}) and 1966 cm^{-1} (ϵ = 703 mm^{-1} M^{-1}), were calculated according to the disappearances of bands at 2006 cm^{-1} (ϵ = 455 mm^{-1} M^{-1}), 1961 cm^{-1} (ϵ = 961 mm^{-1} M^{-1}), and 1794 cm^{-1} (ϵ = 1008 mm^{-1} M^{-1}) ascribed to $Cp_2Fe_2(CO)_4$.

$Cp(CO)_2FeSnBu_3$. A THF solution of $Cp(CO)_2FeNa$ was prepared from 2.1 g (5.9 mmol) of $Cp_2Fe_2(CO)_4$ and sodium amalgam (0.6 g of Na and 60 g of Hg) in 100 mL of THF by stirring the mixture at room temperature overnight.[19] After the mixture was separated from Hg by a cannula to another flask, 3.0 mL (11 mmol) of $ClSnBu_3$ was added. The mixture was then stirred at room temperature for 3 h. The THF was removed by evacuation and the residue extracted with 2 × 200 mL hexane. After filtration, the hexane was evaporated and a red-orange liquid was obtained (~4.5 g). The product was further purified by distillation under reduced pressure (~140 °C at 0.05 mmHg). Anal. Calcd for $C_{19}H_{32}FeO_2Sn$: C, 48.86; H, 6.91; Fe, 11.96; Sn, 25.41. Found: C, 48.54; H, 7.02; Fe, 12.06; Sn, 25.07. IR (ν_{CO}, in hexane): 1989 cm^{-1} (ϵ = 539 mm^{-1} M^{-1}) and 1940 cm^{-1} (ϵ = 606 mm^{-1} M^{-1}).

$Cp(CO)Fe(H)(SnBu_3)_2$. A solution of 0.15 g (0.3 mmol) of $Cp(CO)_2FeSnBu_3$ and 0.11 mL (0.4 mmol) of $HSnBu_3$ in 10 mL

(12) Blaha, J. P.; Bursten, B. E.; Dewan, J. C.; Frankel, R. B.; Rudolph, C. L.; Wilson, B. A.; Wrighton, M. S. *J. Am. Chem. Soc.* **1985**, *107*, 4561.
(13) Zhang, S.; Brown, T. L. *J. Am. Chem. Soc.* **1992**, *114*, 2723.
(14) Labinger, J. A.; Madhavan, S. *J. Organomet. Chem.* **1977**, *134*, 381.
(15) Chang, B.-H.; Coil, P. C.; Brown, M. J.; Barnett, K. W. *J. Organomet. Chem.* **1984**, *270*, C23.
(16) Brunner, H.; Fisch, K. *J. Organomet. Chem.* **1991**, *412*, C11.
(17) (a) Sullivan, R. J.; Brown, T. L. *J. Am. Chem. Soc.* **1991**, *113*, 9155. (b) Sullivan, R. J.; Brown, T. L. *J. Am. Chem. Soc.* **1991**, *113*, 9162.
(18) (a) Davison, A.; McCleverty, J. A.; Wilkinson, G. *J. Chem. Soc.* **1963**, 1133. (b) Fergusson, S. B.; Sanderson, L. J.; Shackleton, T. A.; Baird, M. C. *Inorg. Chim. Acta* **1984**, *83*, L45. (c) Kuzlauskas, R.; Wrighton, M. S. *Organometallics* **1982**, *1*, 602.
(19) (a) Gorsich, R. D. *J. Am. Chem. Soc.* **1962**, *84*, 2486. (b) King, R. B.; Pannell, K. H. *Inorg. Chem.* **1968**, *7*, 1510.

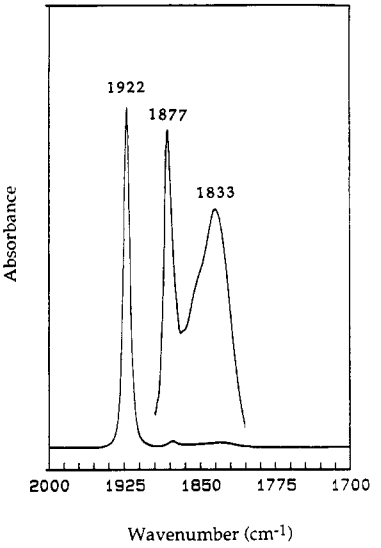

Figure 1. IR spectrum of $Cp(CO)Fe(H)(SnBu_3)_2$ in hexane.

of hexane was photolyzed using a sunlamp for 11 h under Ar. The solution was then taken into the glovebox and passed through a Florisil (Fisher Scientific) column 1.5 cm in diameter, 20 cm long, using hexane as the eluent. Two yellow bands were resolved on the column and collected separately. The solution containing the second band (~20 mL) was worked up by removing the solvent and drying under vacuum. The liquid product was characterized by elemental analysis, NMR and IR spectroscopies. Anal. Calcd for $C_{30}H_{60}FeOSn_2$: C, 49.36; H, 8.28; Fe, 7.65; Sn, 32.52. Found: C, 49.39; H, 8.32; Fe, 7.63; Sn, 32.43. The ^1H NMR spectrum of $Cp(CO)Fe(H)(SnBu_3)_2$ in C_6D_6 shows δ 4.25 ppm (s, 5 H, C_5H_5), δ 0.9–1.8 ppm (m, 54 H, C_4H_9), and δ −13.15 ppm (s, 1 H, FeH). Five peaks were observed on the ^{13}C NMR spectrum at δ 78.9 ppm (C_5H_5) and δ 30.7, 28.1, 15.3, and 14.19 ppm (C_4H_9). The IR spectrum in hexane is shown in Figure 1. In addition to a single CO stretching absorption at 1922 cm^{-1} (ϵ = 385 mm^{-1} M^{-1}), a weak and broad peak at 1833 cm^{-1} (ϵ = 6 mm^{-1} M^{-1}), assignable to Fe–H stretching, was found, together with the ^{13}CO satellite peak at 1877 cm^{-1}.

The reaction minor product (X), obtained from workup of the solution containing the first band (~7 mL) of the column chromatographic separation, shows no CO stretching bands in the IR spectrum (2200–1600 cm^{-1}). The ^1H NMR spectrum in C_6D_6 shows δ 4.24 ppm (s, C_5H_5), δ 0.8–1.9 ppm (m, C_4H_9), and three peaks at δ −16.99, −17.08, and −17.17 ppm (XL200, 200 MHz) in ~1:3:1 relative intensity. It was confirmed that the peaks were *J*-coupled by also taking the spectrum on a 400-MHz instrument (U400). This product contains some impurities (<10%). Further purification and characterization of X was not attempted at this time.

Flash Photolysis. The conventional flash photolysis apparatus, comprising two linear high-pressure xenon-flash tubes and the associated detection system, has been described previously.[17b,20] The cells used in flash photolysis experiments were made of Pyrex glass with optical glass windows. The inner tube of the cells is 8 mm in diameter and 10 cm in length along the probe beam path. The cell temperature was regulated to within 0.2 °C by circulating water from a constant-temperature bath through the jacketed cells. The cells were also fitted with threaded Teflon stopcocks and attached Pyrex bulbs (40 mL) for freeze–pump–thaw degassing of solutions.

Transient absorptions were commonly acquired by using a Markenrich WAAG board. For processes that last longer than 8 s, the voltage changes as a function of time after a flash were measured with a digital voltmeter. Kinetics data were collected on floppy disks and later analyzed by employing ASYST-based computer programs on a Zenith 386SX microcomputer.

(20) (a) Zhang, S.; Dobson, G. R.; Brown, T. L. *J. Am. Chem. Soc.* **1991**, *113*, 6908. (b) Herrick, R. S.; Herrinton, T. R.; Walker, H. W.; Brown, T. L. *Organometallics* **1985**, *4*, 42.

Table I. IR Data for Relevant Compounds in Hexane

compd	ν_{CO}, cm^{-1} (ϵ, mm^{-1} M^{-1})
$Cp_2Fe_2(CO)_4$ (1)	2006 (455), 1961 (961), 1794 (1008)
$Cp(CO)_2FeH$ (2)	2023 (608), 1966 (703)
$Cp(CO)_2FeSnBu_3$ (3)	1989 (539), 1940 (606)
$Cp(CO)Fe(H)(SnBu_3)_2$ (4)	1922 (385)

Table II. Product Distributions for 20-min Photolysis of $Cp_2Fe_2(CO)_4$ (1.5 mM) and $HSnBu_3$ (15 mM) under 1 atm of Ar, Ar/CO, or CO in Hexane

cover gas	Ar	Ar/CO (3:1)	CO
$-\Delta[Cp_2Fe_2(CO)_4]$ (mM)	0.66	0.60	0.53
$[Cp(CO)_2FeH]$ (mM)	0.64	0.61	0.56
$[Cp(CO)_2FeSnBu_3]$ (mM)	0.03	0.10	0.18
$[Cp(CO)Fe(H)(SnBu_3)_2]$ (mM)	0.65	0.52	0.38

To obtain the IR spectra of a solution after flash photolysis, the IR cell was placed between the xenon-flash tubes and then immediately moved to the IR spectrometer following the flash.

Results and Discussion

Continuous Photolysis Study. The photochemical reaction between $Cp_2Fe_2(CO)_4$ and $HSnBu_3$ in hexane was carried out at room temperature under 1 atm of Ar, CO, or Ar/CO gas mixtures. As the reaction proceeds, IR bands at 2006, 1961, and 1794 cm^{-1} due to $Cp_2Fe_2(CO)_4$ (1) decrease in intensity, and three sets of new IR bands are seen: 2023 and 1967 cm^{-1}, assigned to $Cp(CO)_2FeH$ (2); 1989 and 1940 cm^{-1}, assigned to $Cp(CO)_2FeSnBu_3$ (3); 1922 cm^{-1}, assigned to $Cp(CO)Fe(H)(SnBu_3)_2$ (4). These reaction products have been independently synthesized and characterized (vide supra). Depending on the relative concentrations of $Cp_2Fe_2(CO)_4$ and $HSnBu_3$ in the solution and the cover gas atmosphere, the product distribution and the rate of loss of $Cp_2Fe_2(CO)_4$ vary significantly.

A set of IR spectra taken at different times during photolysis of $Cp_2Fe_2(CO)_4$ (0.028 mmol in 10 mL hexane) and $HSnBu_3$ (0.056 mmol) under Ar is shown in Figure 2. Formation of all the products (2–4) was observed in the early stages of the reaction. As the $HSnBu_3$ is consumed, as indicated by the loss of the IR absorption due to Sn–H stretching at 1812 cm^{-1}, the amount of 3 continuously grows; the concentration of 4 has slightly decreased and 2 has completely disappeared when the reaction has been carried out for 2 h.

Figure 3 shows a set of IR spectra from photolysis of $Cp_2Fe_2(CO)_4$ (1.5 mM) and $HSnBu_3$ (15 mM) under Ar, using a 10-fold excess of $HSnBu_3$ over $Cp_2Fe_2(CO)_4$. One can see that formation of 3 is suppressed in the presence of excess $HSnBu_3$.

Under identical conditions of irradiation, photolysis of $Cp_2Fe_2(CO)_4$ (1.5 mM) and $HSnBu_3$ (15 mM) under an Ar, Ar/CO (3:1), or CO atmosphere afforded IR spectra as shown in Figure 4. The difference spectra were taken 20 min after photolysis. The positive peaks are due to formation of the products, while the negative peaks are due to the loss of $Cp_2Fe_2(CO)_4$.

From absorbance measurements on authentic samples (Table I), the product distributions were determined, as shown in Table II. The values in Table II were based on Figure 4 in which absorbance changes at 2006, 2023, 1989, and 1922 cm^{-1} were used for calculation of $-\Delta[Cp_2Fe_2(CO)_4]$ (loss of 1), $[Cp(CO)_2FeH]$, $[Cp(CO)_2FeSnBu_3]$, and $[Cp(CO)Fe(H)(SnBu_3)_2]$, respectively. As seen in Figure 4 and Table II, the rate of loss of 1 is reduced with increases in CO pressure, while the relative amount of 3 formed increases, with a concomitant decrease of 4. However, the $[Cp(CO)_2FeH]$ always appears in a 1:1 ratio with the sum of $[Cp(CO)_2FeSnBu_3]$ and $[Cp(CO)Fe(H)$-

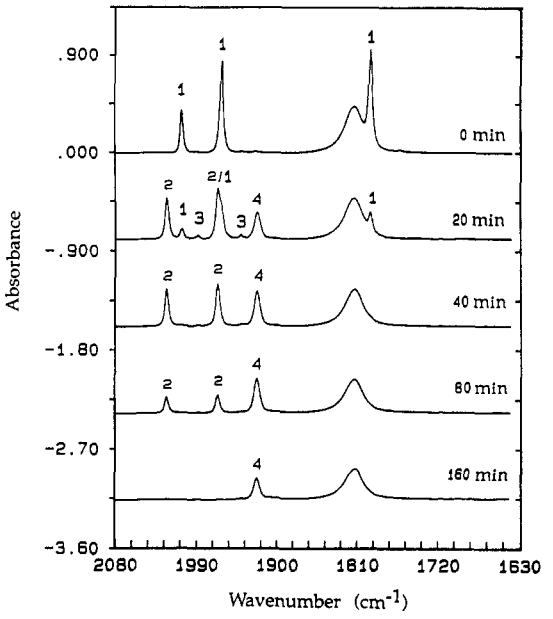

Figure 2. IR spectra taken at different times during photolysis of $Cp_2Fe_2(CO)_4$ (0.028 mmol in 10 mL of hexane) and $HSnBu_3$ (0.056 mmol) under Ar.

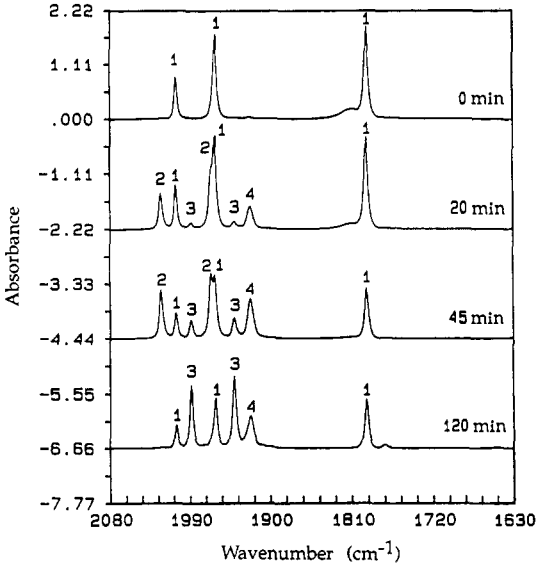

Figure 3. IR spectra taken at different times during photolysis of $Cp_2Fe_2(CO)_4$ (1.5 mM) and $HSnBu_3$ (15 mM) in hexane under Ar.

$(SnBu_3)_2$] and in a 1:1 ratio with $-\Delta[Cp_2Fe_2(CO)_4]$.

The existence of an inverse [CO] dependence and the product distribution rule out the atom-transfer reaction pathway 1. The reactivity of $Cp(CO)_2Fe^\bullet$ toward H atom transfer should not be affected by the presence of CO. For $[Cp(CO)_2FeH]$ and $[Cp(CO)_2FeSnBu_3]$ + $[Cp(CO)Fe(H)(SnBu_3)_2]$ to be in a 1:1 ratio via pathway 1, all the $Bu_3Sn^\bullet$ radicals formed would have to react with $Cp(CO)_2Fe^\bullet$ to form **3**, which would then subsequently react with $HSnBu_3$ to produce **4**. That **4** might be a secondary photolysis product from **3** at this early stage of photolysis is very unlikely. The absorbance due to **3** at the wavelength of interest, notably 366 nm, is not large compared with that of **1** ($\epsilon_{366nm}(1)/\epsilon_{366nm}(3) \approx 5$). Thus a strong internal filter effect operates. Furthermore, the direct photochemical reaction of **3** with $HSnBu_3$ in the absence of **1** is too slow to account for the observations. Flash photolysis experiments discussed below also rule against this possibility.

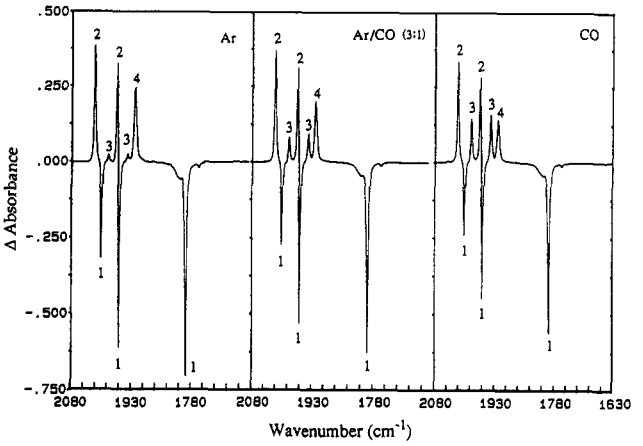

Figure 4. Difference IR spectra taken after photolyzing solutions of $Cp_2Fe_2(CO)_4$ (1.5 mM) and $HSnBu_3$ (15 mM) in hexane for 20 min. The solutions were under an Ar, Ar/CO (3:1), or CO atmosphere.

Scheme I

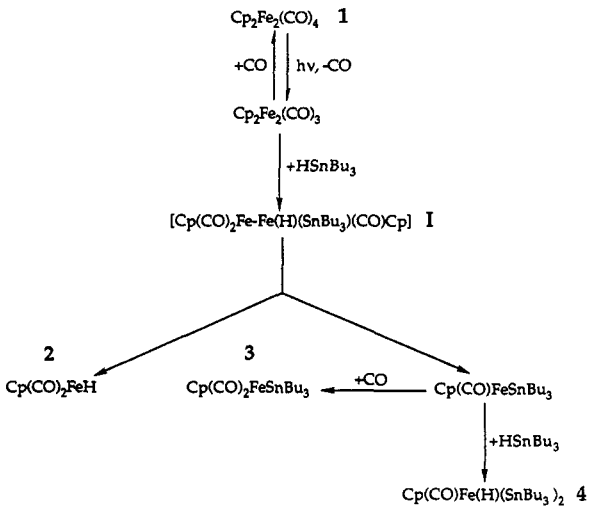

Although pathway 2 seems to account for the observed products in photolysis of $Cp_2Fe_2(CO)_4$ and $HSnBu_3$, the observed product distributions could only arise as an unlikely coincidence. In fact, the observed product distributions contrast with those observed in reactions where pathway 2 was presumed to be operative: reactions of $HSnBu_3$ with $Co_2(CO)_6(PBu_3)_2$ and $Cp_2M_2(CO)_6$ (M = Mo, W), in which only $Bu_3P(CO)_3CoSnBu_3$ and $Cp(CO)_3MSnBu_3$, respectively, were observed as products.[21]

The observations are best accounted for in terms of Scheme I. The proposed reaction mechanism is similar to that put forth to account for the photochemical reaction of $Mn_2(CO)_{10}$ with $HSnBu_3$, in which reaction proceeds via oxidative addition of $HSnBu_3$ to the CO-loss intermediate[17] (pathway 3).

This mechanism is consistent with the observation of CO inhibition of the reaction, via recombination of CO with $Cp_2Fe_2(CO)_3$, and the fact that formation of **2** is in a 1:1 molar ratio with **3** + **4**. The products are all generated from the same intermediate, $[Cp(CO)_2Fe–Fe(Cp)(CO)(H)(SnBu_3)]$ (I), formed via oxidative addition of $HSnBu_3$ to $Cp_2Fe_2(CO)_3$. Reductive elimination of **2** from I creates the unsaturated species $Cp(CO)FeSnBu_3$ which then affords **3** or **4** through competitive reactions with CO or $HSnBu_3$, respectively. The product **4** has not previously

(21) (a) Wegman, R. W.; Brown, T. L. *J. Am. Chem. Soc.* **1980**, *102*, 2494. (b) Wegman, R. W.; Brown, T. L. *Organometallics* **1982**, *1*, 47.

Scheme II

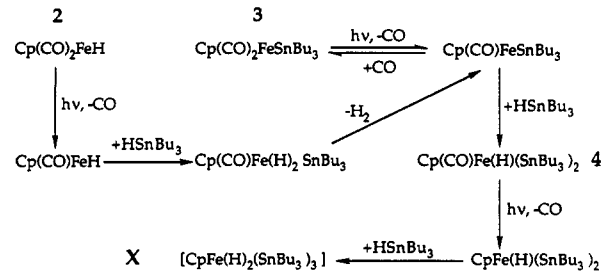

been reported. An analogue of it, $Cp(CO)Fe(H)(SiHPh_2)_2$, has been synthesized recently via a different route and was found to be a catalytically active intermediate in hydrosilation reactions.[16] Another analogue of 4, $(CO)_4Mn(H)(SnBu_3)_2$, was identified as a product, although it proved too unstable to isolate, from photochemical reaction of $Mn_2(CO)_{10}$ with $HSnBu_3$ via a similar reaction pathway.[17] It is noteworthy that no evidence of H to Sn coupling was revealed in the ^1H NMR spectra of either 4 or $(CO)_4Mn(H)(SnBu_3)_2$ (MnH δ −7.5 ppm).

Prolonged photolysis of $Cp_2Fe_2(CO)_4$ and $HSnBu_3$ results in secondary photochemical reactions. Photolysis of 3 with $HSnBu_3$ under Ar produced 4. The disappearance of 2 over prolonged photolysis (Figures 2 and 3) implies further photochemical conversions. Loss of 4 upon extended photolysis (Figures 2 and 3), and the formation of yet another product (X) may suggest further photochemical reaction of 4 with $HSnBu_3$. X exhibits no CO stretching modes in the IR spectrum. The NMR spectra reveal a Cp ring and $SnBu_3$ groups. It also is probably a hydride, as implied by the upfield ^1H NMR chemical shift (δ −17 ppm). One possible structure for X is the dihydrido compound $CpFe(H)_2(SnBu_3)_3$. The observed satellite peaks around δ −17.08 ppm may arise from $^{117}SnFe^1H$ and $^{119}SnFe^1H$ couplings (^{117}Sn 7.6%; ^{119}Sn 8.6%; $I = {}^1/_2$). There is a ~34% probability that one Sn nuclear has spin (giving rise to a doublet) and a ~7% probability that two Sn nuclei have spin (giving rise to a triplet). With the assumption that the coupling constants to ^{117}Sn and ^{119}Sn nuclei are essentially the same and that the protons are magnetically equivalent, the predicted intensity distribution is as observed. The observed coupling constant, 18 Hz, is *not* inconsistent with the proposed structure, that is, with a fully oxidatively added $HSnBu_3$ molecule.[22] Possible reaction pathways leading to the dihydrido species are shown in Scheme II.

Flash Photolysis Results. The CO-loss species $Cp_2Fe_2(\mu\text{-}CO)_3$ and $Cp_2Fe_2(\mu\text{-}CO)2(\mu\text{-}\eta^1,\eta^2\text{-}CO)$, generated upon flash photolysis of $Cp_2Fe_2(CO)_4$, show UV–vis absorption bands at λ_{max} = 510 nm and $\lambda_{max} \approx$ 380 nm, respectively. Under Ar, $Cp_2Fe_2(\mu\text{-}CO)_3$ disappears over a period of about 10 s at room temperature, following a second-order rate law, via recombination with CO. $Cp_2Fe_2(\mu\text{-}CO)2(\mu\text{-}\eta^1,\eta^2\text{-}CO)$ disappears over a period of 2–3 h.[13] However, although it is considerably more stable under Ar, $Cp_2Fe_2(\mu\text{-}CO)2(\mu\text{-}\eta^1,\eta^2\text{-}CO)$ is formed in much smaller amounts.

When $HSnBu_3$ is present in solution, the absorbance due to $Cp_2Fe_2(\mu\text{-}CO)_3$ decays in the millisecond time scale. The concentration of $Cp_2Fe_2(CO)_4$ is typically 3×10^{-5} M and $[HSnBu_3]$ is in the range 5×10^{-4} to 10^{-2} M. The decay

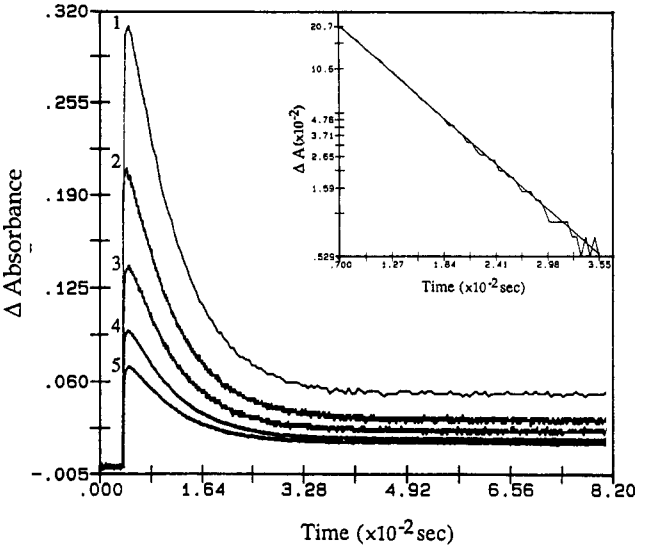

Figure 5. Transient absorbance changes after successive flashes upon a solution of $Cp_2Fe_2(CO)_4$ (0.03 mM) and $HSnBu_3$ (0.98 mM) in hexane under Ar at 25 °C. Inset: plot of ln ΔA ($\Delta A = A_t - A_\infty$) vs time.

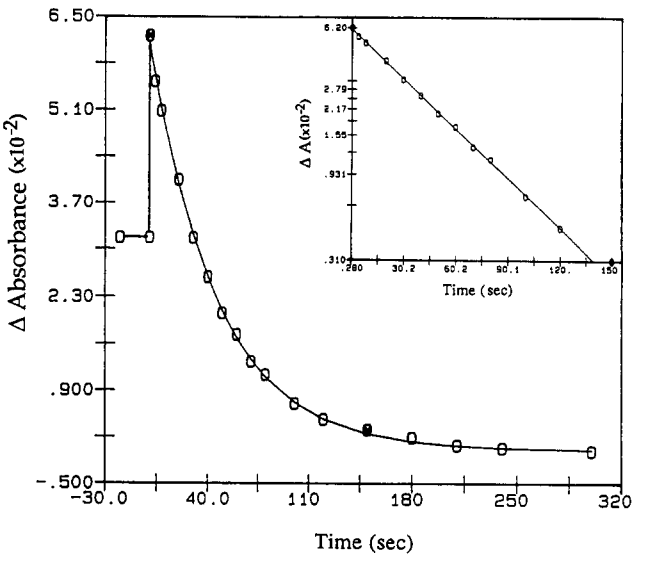

Figure 6. Absorbance change after flash photolysis of a solution of $Cp_2Fe_2(CO)_4$ (0.03 mM) and $HSnBu_3$ (4.0 mM) in hexane under Ar at 25.0 °C. Inset: plot of ln ΔA ($\Delta A = A_t - A_\infty$) vs time.

of $Cp_2Fe_2(\mu\text{-}CO)_3$, as monitored as 510 nm, obeys pseudo-first-order kinetics. Figure 5 shows a set of transient absorbance changes after flash photolysis of $Cp_2Fe_2(CO)_4$ and $HSnBu_3$ (9.8×10^{-4} M) in hexane under Ar at 25.0 °C. These signals, labeled 1–5, correspond to successive flashes on the same solution, with a time interval of 4–10 min between each flash. The first-order behavior is indicated by the linear plot of ln ΔA ($\Delta A = A_t - A_\infty$) vs time for the first trace. As seen from Figure 5, the absorbance change in each flash decreases with increasing number of flashes, indicating that $Cp_2Fe_2(CO)_4$ is consumed with every flash. However, the rate constants calculated from these decays are the same within experimental error. Thus, the reaction products do not interfere with measurement of the rate constant for the reaction of $Cp_2Fe_2(\mu\text{-}CO)_3$ with $HSnBu_3$, nor do they alter its value.

When the transient absorbance change is monitored in an 8-s time scale, the longest time scale available for the Markenrich WAAG board data acquisition, it was found the residual absorbance observed in Figure 5 further decreases. By using a digital voltmeter, the absorbance

(22) (a) Schubert, U. *Adv. Organomet. Chem.* **1990**, *30*, 151. (b) Schubert, U.; Kunz, E.; Harkers, B.; Willnecker, J.; Meyer, J. *J. Am. Chem. Soc.* **1989**, *111*, 2572. (c) Moss, J. R.; Graham, W. A. G. *J. Organomet. Chem.* **1969**, *18*, P24. (d) Faller, J. W.; Johnson, B. V.; Schaeffer, D. C., Jr. *J. Am. Chem. Soc.* **1976**, *98*, 1395.

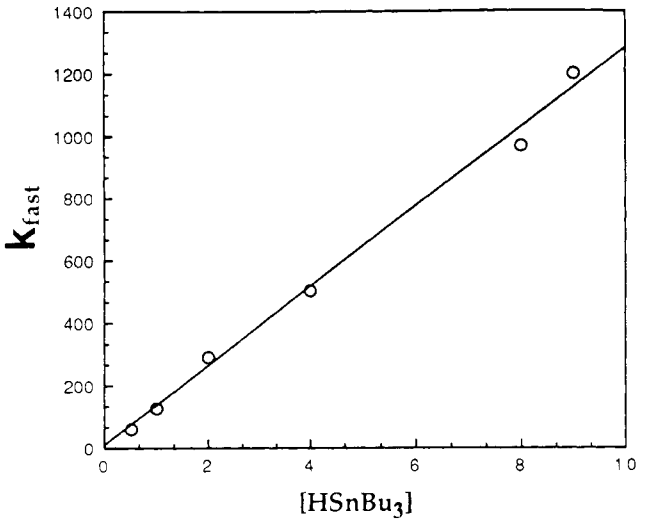

Figure 7. Plot of k_{fast}, the pseudo-first-order rate constant for the disappearance of $Cp_2Fe_2(\mu\text{-}CO)_3$, vs $[HSnBu_3]$.

change over longer times (~300 s) after a flash was calculated on the basis of the voltage measurements. Figure 6 is a plot of ΔA vs time obtained from the flash of $Cp_2Fe_2(CO)_4$ and $HSnBu_3$ (4.0×10^{-3} M) in hexane under Ar at 25.0 °C. The slower process also obeys a first-order rate law, as indicated by the linear plot of ln ΔA vs time shown in the inset. It is noteworthy that the final absorbance lies below the preflash absorbance level.

The rate constants for the faster process, k_{fast}, and for the slower process, k_{slow}, have been determined at various $HSnBu_3$ concentrations, as shown in Table III. A linear dependence of k_{fast} on $[HSnBu_3]$ was observed, as illustrated in Figure 7. The second-order rate constant, calculated from the slope of the plot of k_{fast} vs $[HSnBu_3]$, 1.26 (±0.04) $\times 10^5$ M^{-1} s^{-1} (25.0 °C) is very close to that of the reaction of $Cp_2Fe_2(\mu\text{-}CO)_3$ with PBu_3 (1.25×10^5 M^{-1} s^{-1}, 24.6 °C) and PPh_3 (2.1×10^5 M^{-1} s^{-1}, 24.7 °C) in cyclohexane.[11c] However, k_{slow} is independent of $[HSnBu_3]$ over the large range of concentrations (1.2×10^{-3} to 3.1×10^{-1} M), with k_{slow} (average) = 2.0 (±0.1) $\times 10^{-2}$ s^{-1}. It is thus likely that the slower process corresponds to a unimolecular reaction of the intermediate (I, Scheme I) generated via

Table III. Rate Constants Obtained From Flash Photolysis of $Cp_2Fe_2(CO)_4$ and $HSnBu_3$ under Ar in Hexane at 25.0 °C

$[HSnBu_3]$ (mM)	$10^{-2}k_{fast}$ (s^{-1})	$[HSnBu_3]$ (mM)	10^2k_{slow} (s^{-1})
0.51	0.632 ± 0.017	1.2	1.8 ± 0.2
0.98	1.30 ± 0.01	4.0	2.1 ± 0.1
2.0	2.88 ± 0.05	6.1	1.8 ± 0.5
4.0	5.01 ± 0.11	8.0	2.0 ± 0.1
8.0	9.67 ± 0.16	31	2.1 ± 0.1
9.0	12.0 ± 0.5	150	1.9 ± 0.1
		310	2.0 ± 0.1

oxidative addition of $HSnBu_3$ to $Cp_2Fe_2(\mu\text{-}CO)_3$ in the faster process.

Since the long-lived intermediate persists over several minutes, it was possible to obtain its IR spectrum. A single FTIR scan can be acquired within 30 s after flash photolyzing a solution in an IR cell. Figure 8 displays the difference IR spectra before and after a single flash on a solution of $Cp_2Fe_2(CO)_4$ (1.5 mM) and $HSnBu_3$ (15 mM) in hexane under Ar or Ar/CO (3:1) mixture. At 30 s after the flash, new IR bands due to 2–4 are seen. In addition, bands at 1991 and 1928 cm^{-1}, although obscured, were also observed and are labeled I in Figure 8. At 160 s after the flash, the spectrum has evolved so that bands due to I have disappeared while those of 2–4 have increased in intensity. It is clear that in the presence of added CO, more **3** has formed during this period of time at the expense of **4**. Since this process occurs after the flash, formation of 2–4 cannot be due to secondary photolysis. These results not only are consistent with those from flash photolysis using visible detection but also strongly support the reaction mechanism proposed in Scheme I.

Our observations demonstrate that the product of initial oxidative addition of $HSnBu_3$ to $Cp_2Fe_2(\mu\text{-}CO)_3$ persists for an extended period before going on to form the observed products. In the absence of direct evidence regarding the detailed nature of the bonding of $HSnBu_3$ to $Cp_2Fe_2(\mu\text{-}CO)_3$, the structure of intermediate I is assumed to be $[Cp(CO)_2Fe\text{–}Fe(H)(SnBu_3)(CO)Cp]$ (eq 14), on the

$$Cp_2Fe_2(\mu\text{-}CO)_3 + HSnBu_3 \underset{}{\overset{k_{fast}}{\rightleftharpoons}} Cp(CO)_2Fe\text{–}Fe(H)(SnBu_3)(CO)Cp \quad (14)$$

basis of the absence of a typical bridging CO stretching

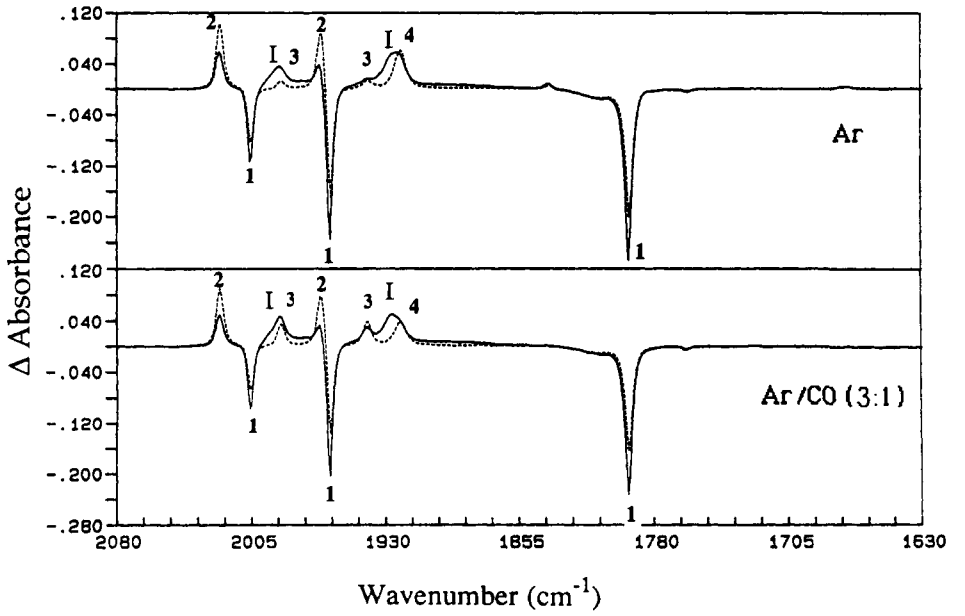

Figure 8. Difference IR spectra taken 30 s (—) and 160 s (- - -) after flash photolysis of solutions of $Cp_2Fe_2(CO)_4$ (1.5 mM) and $HSnBu_3$ (15 mM) in a 1-mm KCl IR cell. The solutions were under an Ar or Ar/CO (3:1) atmosphere.

band in the IR spectrum. The experimental evidence supports the reductive elimination of $Cp(CO)_2FeH$ (eq 15)

$$Cp(CO)_2Fe\text{–}Fe(H)(SnBu_3)(CO)Cp \xrightarrow{k_{slow}} Cp(CO)_2Fe(H) + Cp(CO)FeSnBu_3 \quad (15)$$

rather than the alternative reductive elimination of $Cp(CO)_2FeSnBu_3$ from I (cf. eq 13). Furthermore, the reductive elimination of $HSnBu_3$ from I is not important (eq 14), as indicated by the fact that k_{slow} is independent of $[HSnBu_3]$.[23]

Under Ar in the presence of $HSnBu_3$, $Cp_2Fe_2(\mu\text{-}CO)_2(\eta\text{-}\eta^1,\eta^2\text{-}CO)$ is observed via very weak peaks at 1839 and 1674 cm^{-1}. It appears that reaction of $HSnBu_3$ with $Cp_2Fe_2(\mu\text{-}CO)_2(\mu\text{-}\eta^1,\eta^2\text{-}CO)$ is much slower than with $Cp_2Fe_2(\mu\text{-}CO)_3$.

The kinetics of oxidative addition of $HSnBu_3$ to $Cp_2Fe_2(\mu\text{-}CO)_3$ are not inconsistent with an associative pathway, as suggested for the reaction of $Cp_2Fe_2(\mu\text{-}CO)_3$ with other ligands.[11c,24] However, it has been demonstrated that reaction of $Mn_2(CO)_7L_2$ (L = PR_3; R = alkyl) with $HSnBu_3$ involves the bridge-on–off equilibrium between the species with a semibridging CO, $Mn_2(CO)_6L_2(\mu\text{-}\eta^1,\eta^2\text{-}CO)$, and a nonbridging species, $L(CO)_4Mn\text{–}Mn(CO)_3L$; the bridging form predominantes, but only the bridge-off form reacts rapidly with $HSnBu_3$.[17] The apparent rate constants, 2.5×10^6 and 3×10^5 M^{-1} s^{-1}, for addition of L = CO and PMe_3, respectively, are close to that for addition of $HSnBu_3$ to $Cp_2Fe_2(\mu\text{-}CO)_3$. At this point it is not clear whether a bridge-on–off equilibrium precedes addition of the ligand to $Cp_2Fe_2(\mu\text{-}CO)_3$. Further study of the reactions of $Cp_2Fe_2(\mu\text{-}CO)_3$ with various nucleophiles is presently underway.

Acknowledgment. This research was supported by the National Science Foundation through Grant CHE89-12773.

OM9108107

(23) It was noted that diffusion processes occur on the time scale of minutes after flash photolyzing a solution in an IR cell. A portion of the solution in the cell is not exposed to the windows and thus is not photolyzed. Diffusion leads to a mixing of exposed and unexposed solution in the window area. The net effect in a difference spectrum, such as shown in Figure 8, is a decrease in absolute magnitudes of both negative and positive peaks. Thus, the observed partial recovery of 1 between 30 and 160 s after the flash does not necessarily indicate that reductive elimination of $HSnBu_3$ to form $Cp_2Fe_2(\mu\text{-}CO)_3$, followed by combination with CO, is occurring. In fact, such a process is expected to be unimportant under the employed reaction conditions, i.e., high $HSnBu_3$ concentration and low CO concentrations in the solution.

(24) Bursten, B. E.; Mckee, S. D.; Platz, M. S. *J. Am. Chem. Soc.* **1989**, *111*, 3428.

Reactions of the Unsaturated Species $(\eta\text{-}C_5Me_5)Ni\text{–}W(CO)_3(\eta\text{-}C_5H_5)$ and of Its Methylene Derivative $(\eta\text{-}C_5Me_5)Ni(\mu\text{-}CO)(\mu\text{-}CH_2)W(CO)_2(\eta\text{-}C_5H_5)$ with Two-Electron Donors

Michael J. Chetcuti,* Kathryn J. Deck, John C. Gordon, and Brian E. Grant

Department of Chemistry and Biochemistry, University of Notre Dame, Notre Dame, Indiana 46556

Phillip E. Fanwick

Department of Chemistry, Purdue University, West Lafayette, Indiana 47907

Received November 4, 1991

The unsaturated complex $(\eta\text{-}C_5Me_5)Ni\text{–}W(CO)_3(\eta\text{-}C_5H_5)$ reacts with two-electron donor ligands or their precursors to afford compounds of generic formula $(\eta\text{-}C_5Me_5)Ni(\mu\text{-}CO)(\mu\text{-}L)W(CO)L'(\eta\text{-}C_5H_5)$ (L = CO; L' = CO, PMe_3, PMe_2Ph, $P(OMe)_3$, PPh_2Cl, PPh_2H. L = ^{t}BuNC, CH_2; L' = CO). The structure of the $\mu\text{-}CH_2$ species $(\eta\text{-}C_5Me_5)Ni(\mu\text{-}CO)(\mu\text{-}CH_2)W(CO)_2(\eta\text{-}C_5H_5)$ (**2**), which has been communicated (Chetcuti, M. J.; Grant, B. E.; Fanwick, P. E. *Organometallics* **1990**, *9*, 1345), has the same molecular geometry as that adopted by most of the other complexes described and is discussed in more depth here. Complex **2** crystallizes in the triclinic space group $P\bar{1}$, with a = 8.518 (2) Å, b = 10.280 (1) Å, c = 10.719 (1) Å, α = 89.26 (1)°, β = 87.24 (1)°, γ = 79.18 (1)°, V = 920.9 (4) Å^3, Z = 2, and was refined to R = 0.039, R_w = 0.053. All complexes exhibit dynamic behavior on the NMR time scale that can be rationalized in light of their observed structures. The phosphine ligands PMe_3 and PPh_2H displace a carbonyl ligand in $(\eta\text{-}C_5Me_5)Ni(\mu\text{-}CO)(\mu\text{-}CH_2)W(CO)_2(\eta\text{-}C_5H_5)$ to afford cis and trans isomers of the phosphine derivatives $(\eta\text{-}C_5Me_5)Ni(\mu\text{-}CO)(\mu\text{-}CH_2)W(CO)L(\eta\text{-}C_5H_5)$ (L = PMe_3, PPh_2H). The reaction of $(\eta\text{-}C_5Me_5)Ni\text{–}W(CO)_3(\eta\text{-}C_5H_5)$ with PPh_2Cl proceeds to give the initial phosphine adduct $(\eta\text{-}C_5Me_5)Ni(\mu\text{-}CO)_2W(CO)(PPh_2Cl)(\eta\text{-}C_5H_5)$. Oxidative addition then ensues to afford the cis species $(\eta\text{-}C_5Me_5)Ni(\mu\text{-}CO)(\mu\text{-}PPh_2)W(CO)Cl(\eta\text{-}C_5H_5)$, which subsequently equilibrates with the trans isomer. PPh_2H is believed to behave similarly, but oxidative addition products are not isolable here. The behavior of the related saturated cyclopentadienylnickel complexes $(\eta\text{-}C_5H_5)(OC)Ni\text{–}W(CO)_3(\eta\text{-}C_5H_4R)$ (R = H, Me) toward PMe_3, PPh_2H, and ^{t}BuNC is discussed. The syntheses of $(\eta\text{-}C_5Me_5)Ni(\mu\text{-}CO)_2Mo(CO)(PPh_2H)(\eta\text{-}C_5H_4Me)$ (Ni–Mo) and of $(\eta\text{-}C_5H_5)Ni(\mu\text{-}^t\text{BuNC})(\mu\text{-}CO)Mo(CO)_2(\eta\text{-}C_5H_4Me)$ (Ni–Mo) are also described.

Introduction

The chemistry of homobimetallic unsaturated compounds toward 2-electron donor ligands is quite variable.[1] In some instances, simple addition to afford 1,2-addition product results. Occasionally the outcome is metal–metal bond cleavage, while, in other cases, there is no reaction at all. A few examples demonstrate that the product obtained is not always predictable. Thus, the complex $Re_2(\mu\text{-}CO)_3(\eta\text{-}C_5Me_5)_2$ (Re≡Re) is unreactive toward

(1) Winter, M. J. *Adv. Organomet. Chem.* **1989**, *29*, 101, and cited references.

0276-7333/92/2311-2128$03.00/0